Marshall Plan Scholarship

Final Report

Andreas Pospischil

January 15 to May 15, 2015
Graduate School of Arts and Sciences, Department of Electrical Engineering, Xia Group
Yale University, New Haven, CT
http://www.eng.yale.edu/xialab

Marshallplan-Jubiläumsstiftung
Austrian Marshall Plan Foundation

Yale

Preface

This document contains unpublished scientific data and must not be published in any way (digital or printed) without permission from the author. Please contact Andreas Pospischil before publishing any parts or figures of this report per mail (andreas.pospischil@tuwien.ac.at).

Introduction

This document summarizes the work, which was performed and subsequent results that were achieved during my visit at Xia-Group at Yale University in 2015.

Research for my PhD study deals with optoelectronics, using a new class of so called two-dimensional materials. These materials, which are as thin as one atomic layer, are a hot topic in many scientific disciplines in recent years and enable to study physical phenomena that were not accessible before their discovery.

My work in Yale concentrated on two-dimensional systems, too. Another material of this class, black phosphorus, was rediscovered in 2014 and is a hot topic in the scientific community since then. It is, like many other two-dimensional materials, a semiconductor, but it happens to have a much smaller bandgap than its counterparts. This enables researchers to create new devices based on black phosphorus like transistors, photodetectors and light emitters.
My task in Yale was to build a photocurrent scanning setup and program the measurement software for the setup and subsequent the fabrication and characterization of different devices.

This report first gives an introduction on two-dimensional materials with a focus on graphene and black phosphorus. The following two chapters deal with the optical setup, the software, which was written, and the results that were obtained in three different projects. At the end, the work is summarized and a brief outlook points out how the work on those projects could go on.

Table of Contents

Background

Graphene, a two-dimensional (2D) layer of carbon atoms arranged in a honeycomb lattice, attracts a lot of attention in the scientific community in recent years. Single layer graphene was first fabricated and studied by Novoselov and Geim, who were awarded with the Nobel prize in physics in 2010 [1,2]. The material has a set of unique physical properties. It is not only the strongest material known to man [3] and harder than diamond, it is also a much better conductor than copper and aluminum [4] and, because of its thinness, graphene is bendable. Moreover, graphene has some stunning properties for optoelectronic and photonic applications. One is the constant absorption of light of 2.3% over a very broad spectral range reaching from the infrared to the ultraviolet, which is due to the gap-less dispersion of the Dirac electrons [5].
With this new material combining all these supreme properties, groundbreaking experiments have been performed. Graphene transistors with f_T of 300 GHz were demonstrated and complete logic circuits, fabricated from CVD grown graphene sheets, have been shown [6,7]. In photonics, the high carrier mobility and broadband absorption is used in ultrafast photodetectors [8] and modulators [9].

Soon it became clear that graphene is not the only 2D material that is provided by nature. A range of other crystals with the same structure as graphite, namely strong atomic bonding within the crystal plane and week van-der-Waals bonding between the planes, are available. These crystals from the transition-metal dichalcogenide (TMDC) group have different physical properties, some being semi-metallic (e.g. $NiTe_2$), or superconducting (e.g. $NbSe_2$, $NbTe_2$), others are semiconducting (e.g. MoS_2, $MoSe_2$, WSe_2, WS_2) or insulating (e.g. h-BN, HfS_2) [10].

Phosphorene, a single layer of black phosphor, is, besides graphene, the second stable monoatomic layered material that is known up to now. Single layers can be produced by mechanical exfoliation from bulk black phosphorus. Phosphorene has, unlike graphene, a direct bandgap, which can be adjusted by the layer number (0.3 eV in bulk, values for a single layer vary in different first-principle calculations from 1 eV to 2 eV) [11,12].

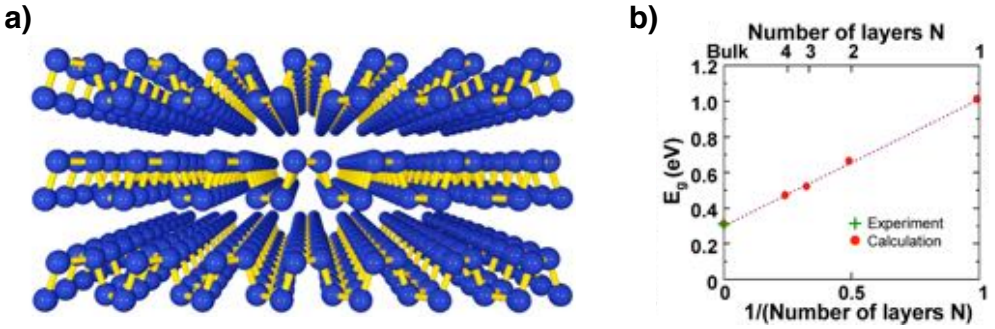

Figure 1: ***(a)*** *Crystal structure of few-layer phosphorene.* ***(b)*** *Calculated bandgap for single and few layer phosphorene (DFT-method) [11].*

The electrical properties of multilayer black phosphorus have been studied very recently by different groups [11-14] (see Figure 2). Multilayer devices (3-60 layers) typically show asymmetric characteristics with higher p-type conductance, meaning a more efficient hole injection into the channel. Moreover, a strong anisotropy along different directions of the crystal is observed leading to an almost doubled Hall mobility value at low temperatures (1000 cm^2/Vs in the light effective mass direction, compared to 600 cm^2/Vs in the heavy mass direction). Black phosphorus thin film transistors exhibit a high on-off ratio exceeding 10^5, field-effect mobility of up to 250 cm^2/Vs and good saturation properties at room temperature. All these properties could lead to a bright future for phosphorene in future high-performance thin film electronics.

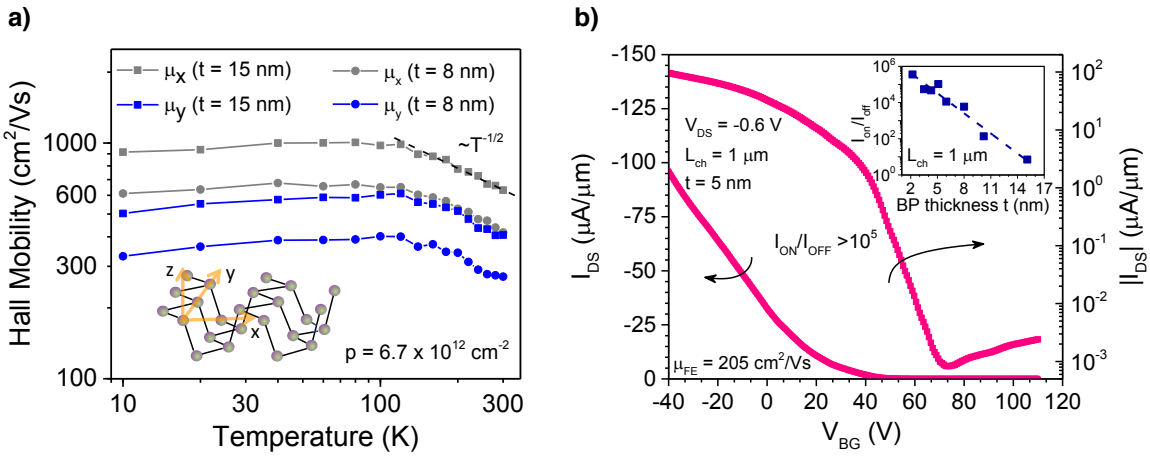

Figure 2: (a) *Hall-mobilities for different directions (x and y) along the crystal. Values are almost doubled in x-direction.* ***(b)*** *Typical transfer characteristic of a black phosphorus thin film transistor. The inset shows the on/off ratio for different flake thickness [14].*

Measurement setup and software

One of the first tasks was to build a scanning photocurrent setup and write measurement software to control it.

Optical setup

The measurement setup looks in principle as follows: 2 different laser sources, a 532 nm and a tunable source with a center frequency around 1550 nm can be coupled through a beamsplitter and a piezo-electric driven scanning mirror into an objective lens. The objective lens focuses the laser beam to a spot with a size of about 1 micrometer for the green laser and about 2 micrometer for the near-infrared source onto the sample.

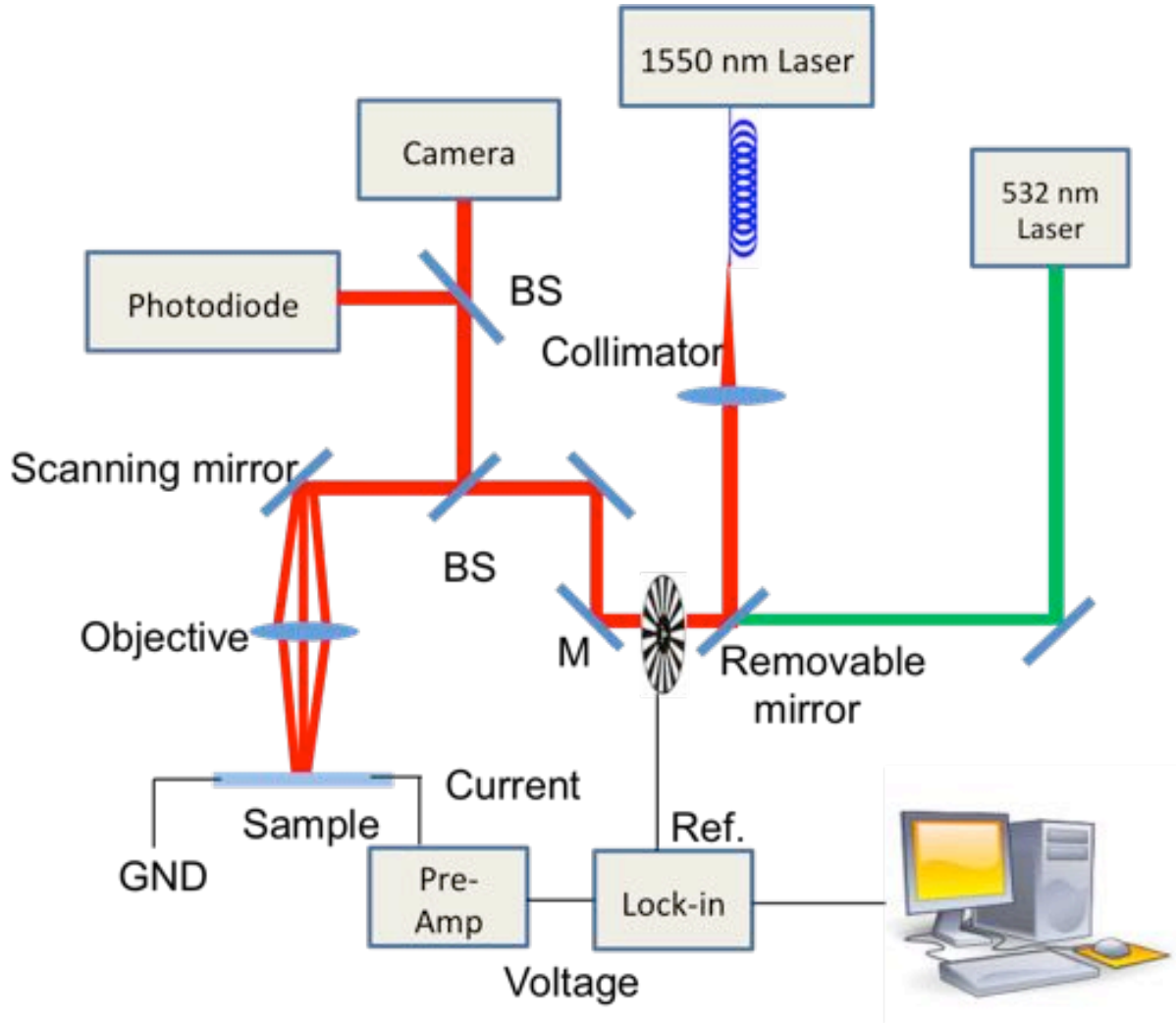

Figure 3: *Sketch of the photocurrent scanning setup including all relevant parts.*

Photocurrent scanning is done in two steps. First, a reflection image of the actual device is taken. Therefore, light, that is reflected by the device (for example gold contact have higher reflection than silicon substrates) is collected by the objective lens and guided via the scanning mirror and the beamsplitters to a photodiode. The photocurrent generated by the photodiode is measured and analyzed by the software, which is also used for photocurrent measurements on the actual device. After thoroughly determining the scanning area by reflection measurements, the same area is scanned again, but this time the photocurrent generated by the device under test is analyzed. In most cases the

photocurrent is small and a transimpedance-preamplifier is used. By using a modulated signal (which means that the laser beam is chopped by a rotating metal blade) and a lock-in amplifier the signal-to-noise ratio can be further increased.

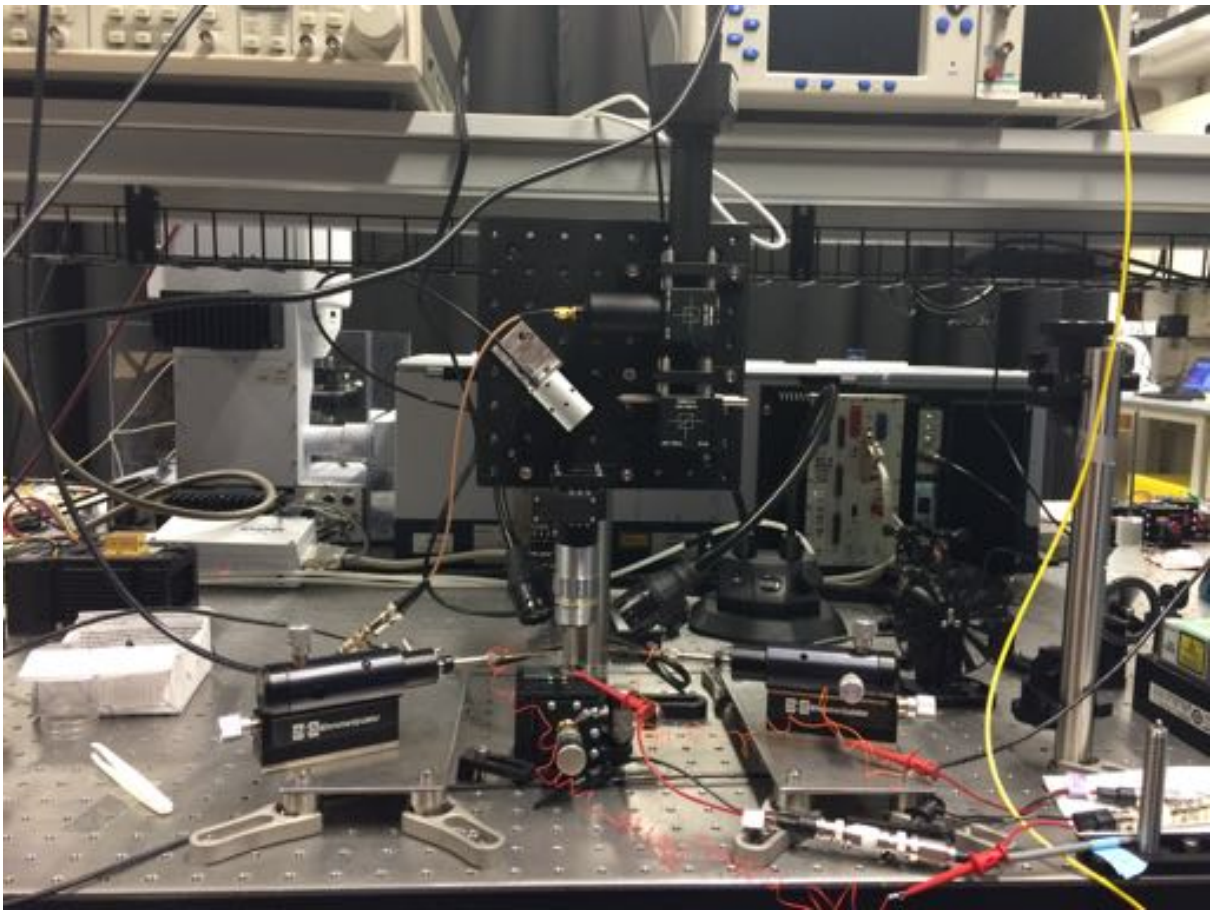

Figure 4: *Photograph of the actual scanning setup.*

Measurement software

The measurement software was written in LabView for two reasons. First, the group supplied a framework, which included most data processing subroutines that were needed, and second, LabView drivers are available for all used equipment.

Basically, the software controls a scanning mirror to guide the laser light from point to point and measures the corresponding photocurrent for each point. The scanning mirror is controlled by a DAQ card (NI 6341 DAQ), which translates the software commands to a voltage that is applied to the piezo motors of the mirror (PI S-334 Tip/Tilt Mirror). After the laser is set to the desired position the corresponding photocurrent is read. Therefore, different measurement devices can be chosen. For relatively large photocurrents the DAQ card itself can be used to read the measurements, for more accurate measurements a Keithley 2612 Sourcemeter and a Stanford Research SR-830 Lock-in amplifier were available. The software communicates with the DAQ card via the USB interface and with the K2612 as well as with the SR-830 via the GPIB interface.

Other software was written to make life in the lab easier. Examples include a small interface to control the scanning mirror separately, an I-V scanner to quickly characterize devices electrically or a user interface, which automates a measurement necessary to characterize the plasmon-enhanced mid-infrared graphene photodetector. The following screenshots show a few of the programs I wrote and give a short explanation in the figure caption.

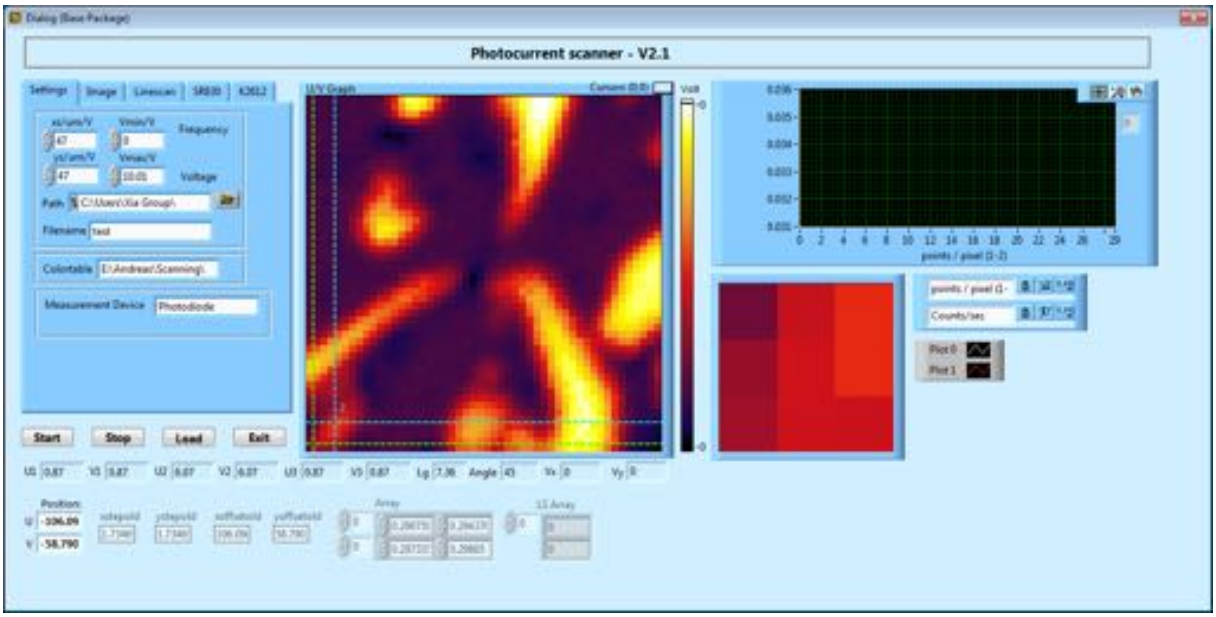

Figure 5: *The photocurrent scanning software. In the 5-tab panel on the left all settings for the scanning mirror as well as for the measurement devices can be found. The main panel in the center shows the measurement results, a reflection measurement in this case. On the right and on the bottom detailed parameters of the actual measurements are shown.*

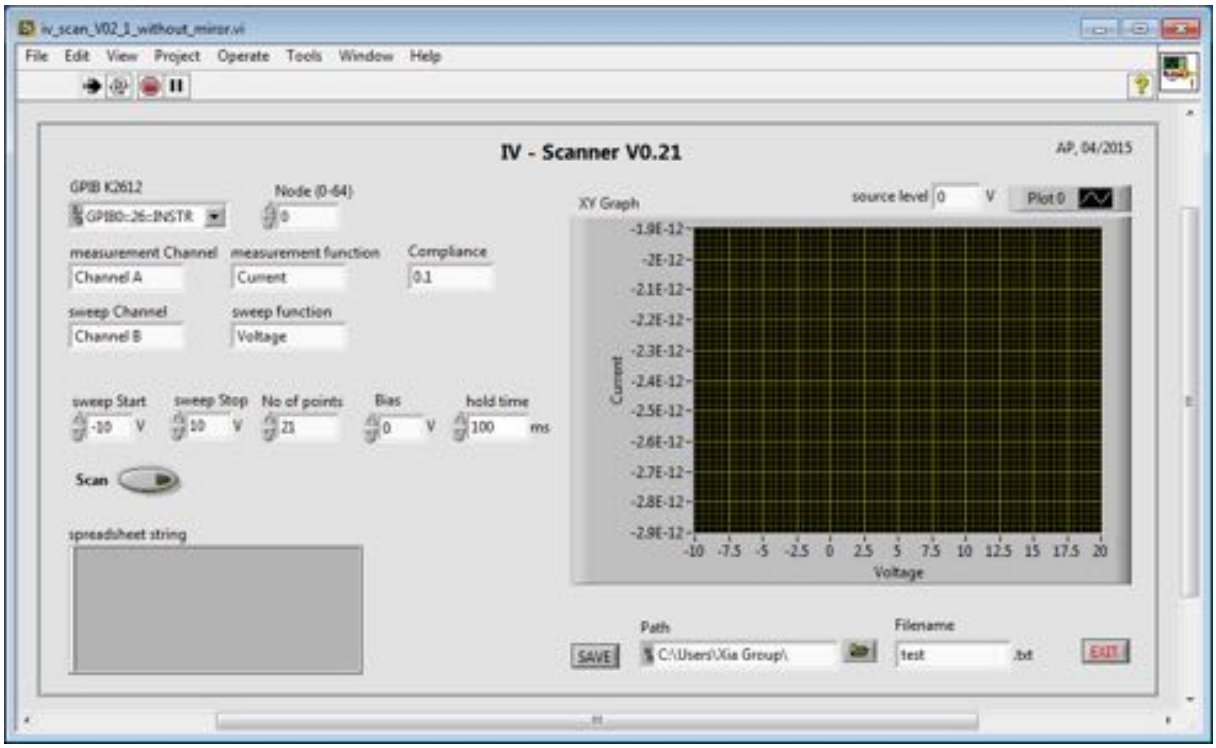

Figure 6: *The IV Scanner is used to electrically characterize our fabricated devices.*

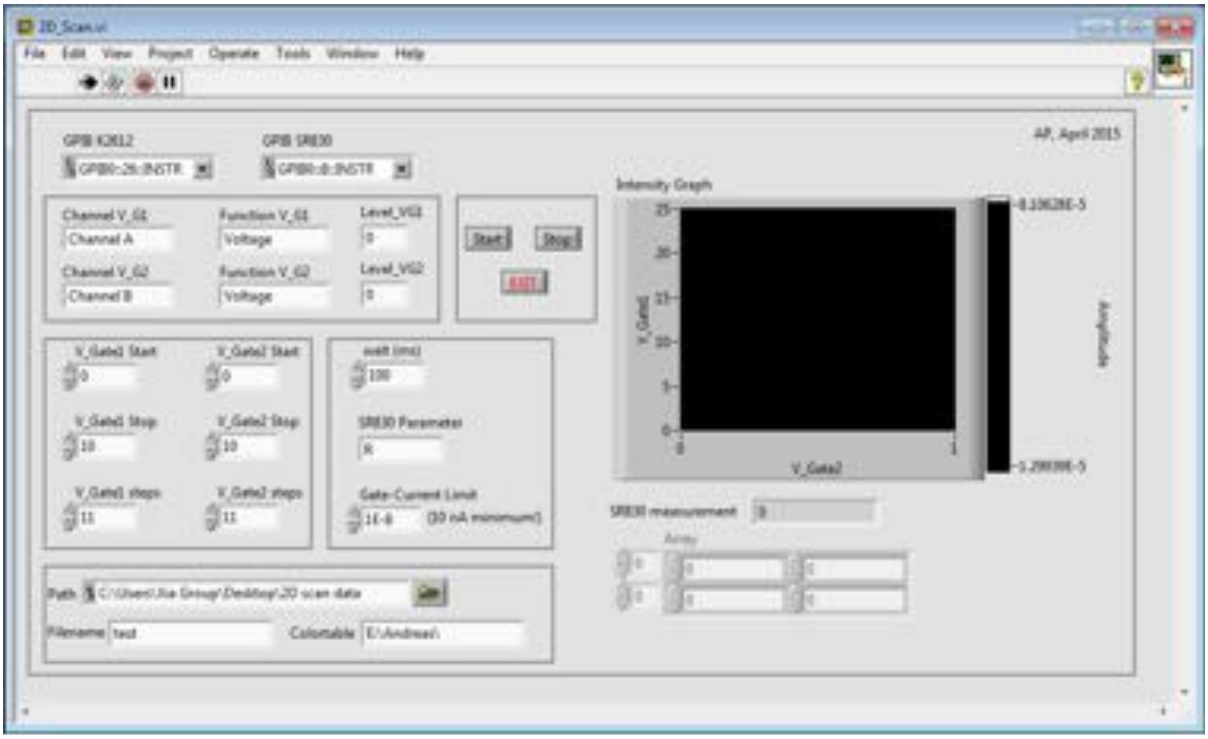

Figure 7: *This software is used to characterize the plasmon-enhanced mid-infrared photodetector. The K2612 controls both gate voltages and the SR830 lock-in amplifier reads the corresponding values for the photocurrent. The result is plotted in the graph on the right.*

Results

I was involved in several projects, working with other members of the research group, especially Dr. Xiaomu Wang, Qiushi Guo and Yichen Jia. We developed and characterized different photodetector device schemes. The results are presented in the next three paragraphs.

Graphene – hBN – Graphene sandwich device

The aim of this project was to confirm the theoretically predicted thermionic emission and negative differential resistance in photoactive graphene heterostructures [15]. The paper suggests, that interlayer transport in graphene heterostructures operating in the hot-carrier regime leads to an unusual type of photoresponse, a negative differential resistance (NDR). "*The mechanism of this NDR response relies on the interplay of two effects. First, the phase space available for phonon scattering rapidly increases with doping, enhancing the electron–lattice cooling and thereby altering the number of hot carriers in the system. Second, the large capacitance of the atomically thin device renders the carrier density in graphene layers sensitive to the interlayer potential difference. These two effects combined together result in a reduction of the electronic temperature and a suppression of thermionic current upon an increase of the bias potential Vb. The NDR effect arises when this suppression overwhelms the increase in the field-effect transport under bias. Such an NDR mechanism manifests itself as an enhanced photocurrent peaked at a bias potential well below the onset of the conventional field-emission regime.*"

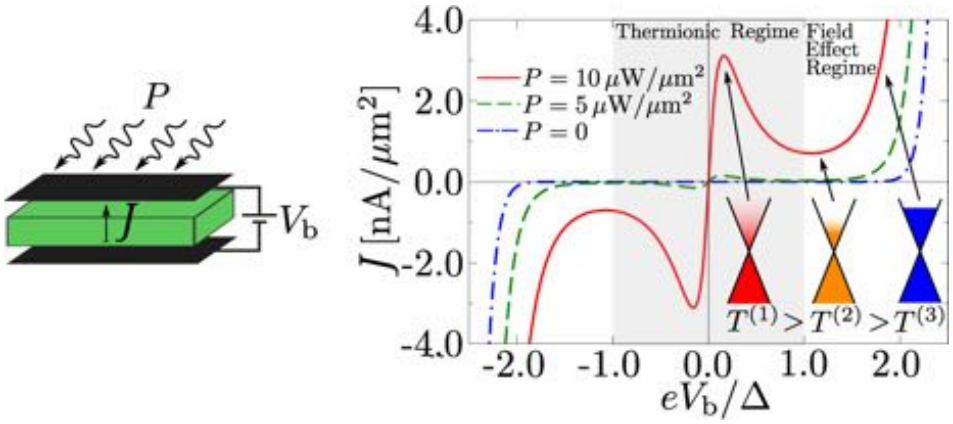

Figure 8: *Device schematics and the IV characteristics under optical pumping. The bias voltage controls the electron cooling through electrostatic doping of graphene layers. An enhancement in the cooling power upon increased bias voltage triggers a carrier temperature drop and leads to negative differential resistance. For larger bias the transport is dominated by field emission.*

Our device consists of 4 nm hexagonal Boron-Nitride (hBN) that is encapsulated by a monolayer of graphene at the top and the bottom. Contacts are made by e-beam lithography and subsequent metal deposition (Ti/Au).

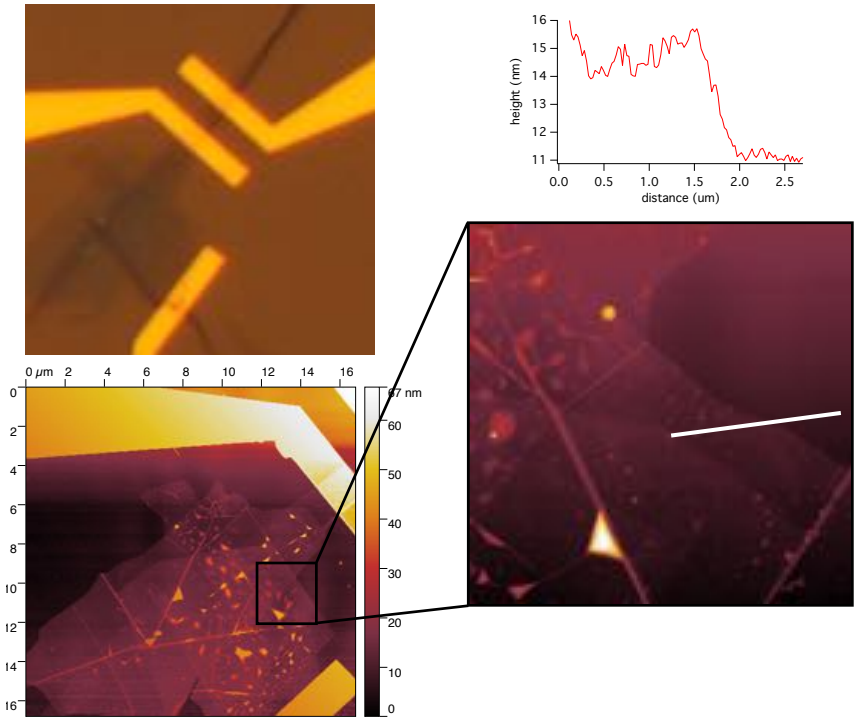

Figure 9: *Optical microscope image of the device as well as AFM measurements to confirm the thickness of the hBN flake. The height profile is taken from the white line indicated in the lower right panel.*

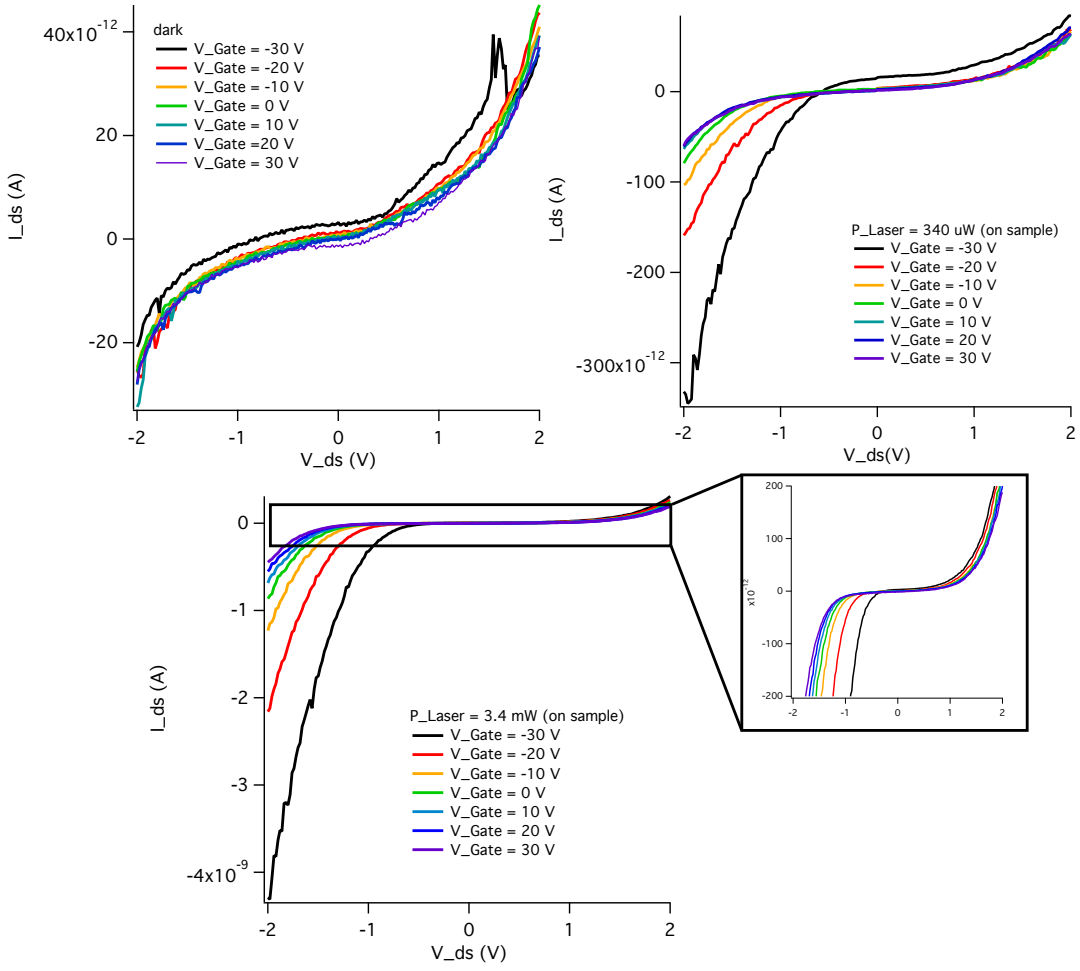

Figure 10: *Electrical characteristics of the G-hBN-G device.*

Figure 10 shows the electrical characteristics under dark (top left) and illuminated conditions. Higher photocurrent is observed for negative V_{DS}, which could be explained by an asymmetry in the device. The bottom figure shows the IV characteristics under high illumination. An increase in photocurrent is observed at lower gate voltages, indicating p-doping of the (bottom) graphene layer.

Although we observed a current increase by a factor of 200 under high illumination there is no indication of negative differential resistance. The increase indicates hot-carrier assisted thermal emission. To observe negative differential resistance a delicate balance between the doping of the two graphene sheets and the bias level must be found.

Future work on this project could include:

- Repeating the measurements at lower temperatures.
- Uniform illumination of the whole device either through reduction of the overlapping region of the device by etching or by defocusing the laser beam. This should exclude a superposition of thermionic emission and „normal“ field emission.
- Fabricate cleaner samples.
- Fabricate samples with different hBN thickness (1 to 10 nm) to compare results.

BP-Si mid-infrared photodetector

The aim of this photodetector is to detect light in the mid-infrared range of the electromagnetic spectrum by exploiting charge-carrier generation at the interface between silicon and black phosphorus. Therefore, a thin film of black phosphorus was transferred onto an n-doped silicon wafer. The wafer is covered with 100 nm silicon dioxide, and windows are opened using wet chemistry. Figure 11 shows a microscope image of the device. On the upper left side the opened silicon windows can be seen between two predefined metal electrodes. The electrodes are used to contact the black phosphorus (the other contact is established by the silicon) and also to probe the device with micro-tips. The upper right shows an image of a thin (30 nm) flake of black phosphorus, which was transferred on a structure described before.

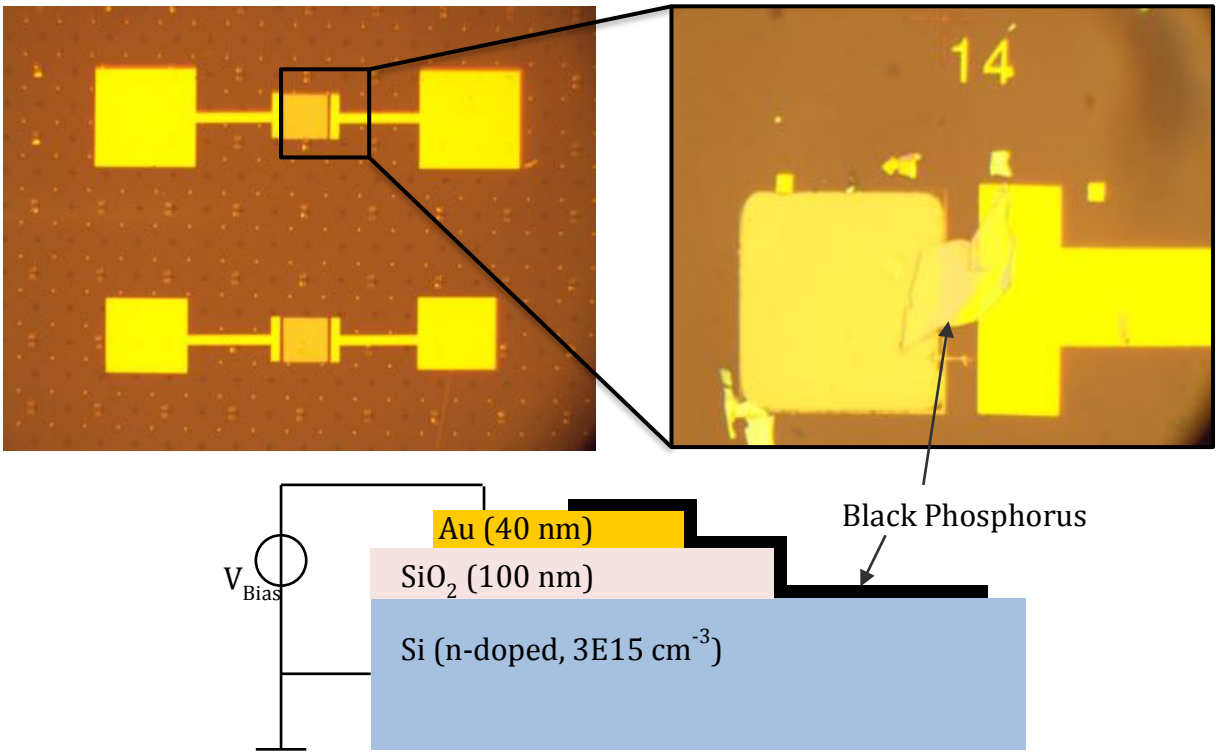

Figure 11: *The upper panels show microscope images of fabricated BP-Si photodetectors. A window was opened on Si wafers covered with thermally grown SiO2 and metal electrodes were patterned before a thin flake of black phosphorus was transferred to the structure. The schematic drawing on the lower side shows the electrical connection.*

The schematic drawing at the bottom of Figure 11 shows the electrical wiring. The silicon itself is used as source, the metal electrode is used as drain, respectively. A bias voltage V_{Bias} is applied between source and drain.

Figure 12 shows the first electrical measurements - the left and the right panel show the same measurement for two different devices. It can be clearly seen that BP on Si forms a rectifying junction in both cases.
If light from a white light source shines on the device, a change in the I-V characteristics can be observed. Under negative bias an increase in current suggests the generation of photo-excited carriers. As we used white light, it can't be distinguished between absorption in BP or silicon. To clarify this, further measurements must be carried out using light with energy lower than the bandgap energy of silicon. As the bandgap of the thin BP is much lower than the bandgap of silicon, absorption in silicon can be excluded in this way.

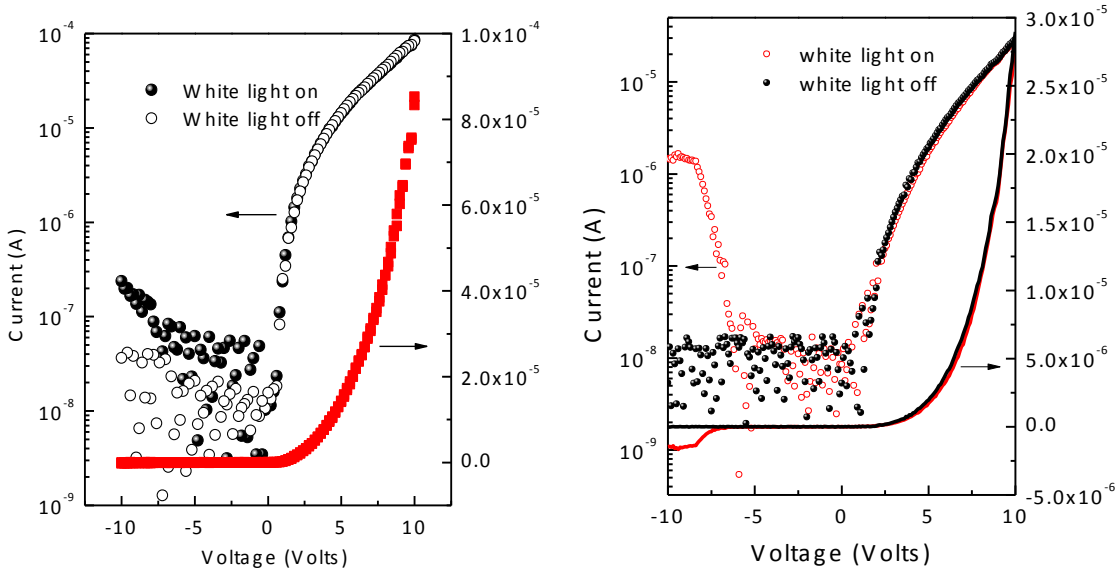

Figure 12: *First electrical characterization of the BP-Si photodetector. The two panels show the same measurement for two different devices, using different BP thickness.*

Figure 13 shows photocurrent measurements using a broadband mid-infrared source. Therefore, the device was mounted on the sample stage of an infrared-microscope and light from a globar was focused onto the device. The result shows photocurrent generated by the device. By rotating the polarization of the light we expect to see a change in the photocurrent, as BP is strongly dependent on the polarization of the incident light [16]. The measurements did not show any dependence on the polarization though. We attribute this to the fact that the mid-infrared source emits a small portion of light, which can again be detected by silicon itself (see spectrum of the mid-infrared source on the right side of Figure 13).

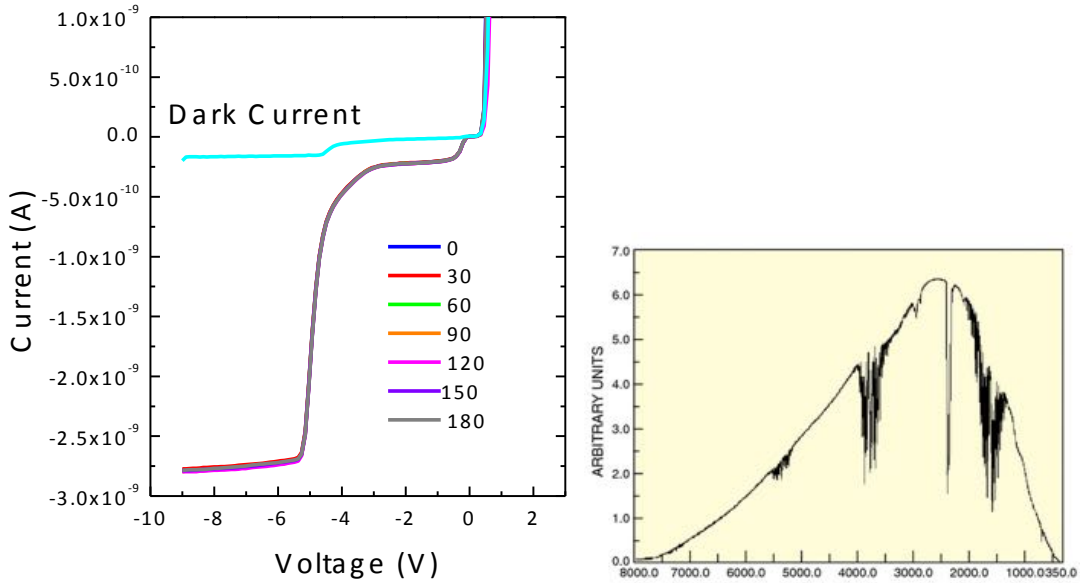

Figure 13: *Photocurrent measurement using a broadband mid-infrared light source. The spectrum of the emitted light is shown in the right panel. We expect to see a change in photocurrent by rotating the polarization of the incident light, as BP is highly anisotropic. As there is no such polarization-dependence we attribute the photocurrent again to silicon-absorption as a small portion of the light has enough energy to be absorbed by silicon.*

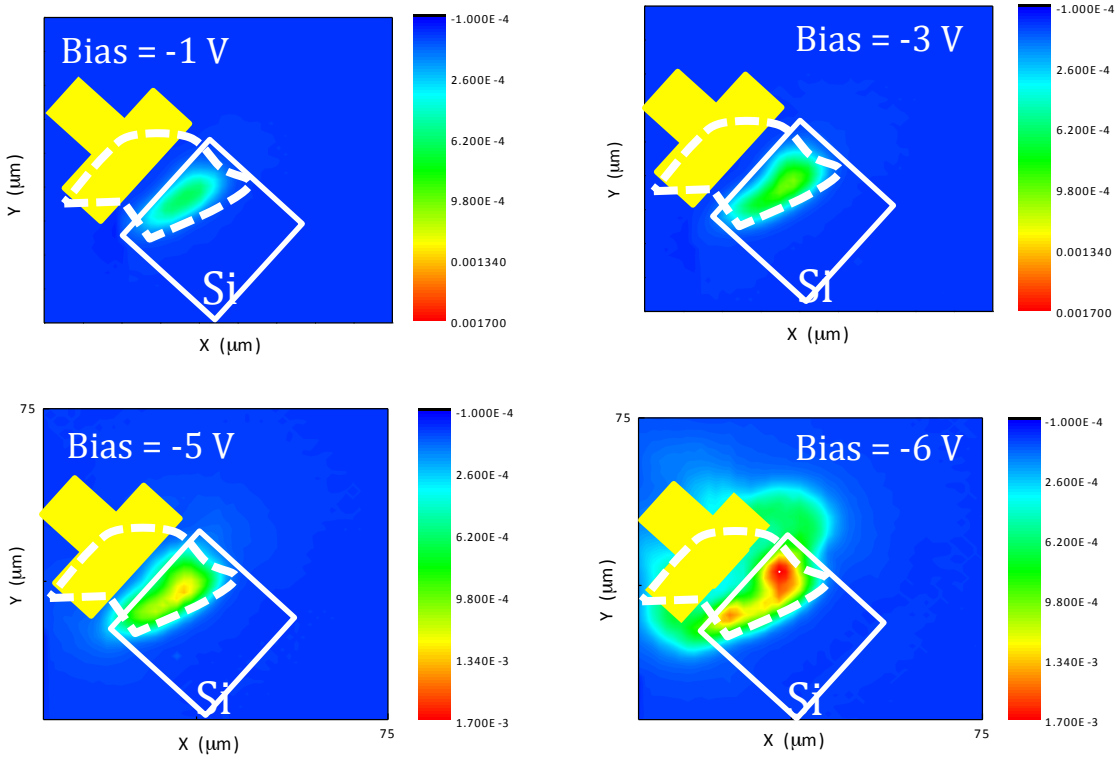

Figure 14: *Photocurrent scanning study of the BP-Si photodetector. Green light with low power (P_{Laser} = 30uW @ 532 nm) was used for this measurement. An increase is observed for higher bias voltage. The photocurrent generation is attributed to silicon-absorption.*

We also performed measurements using a laser with a wavelength of 1.55 micrometer to exclude absorption in silicon. Against all expectations we could not get any results, meaning no photocurrent was generated. This is counterintuitive for two reasons. First, a paper by Youngblood et al. [17] confirms absorption of 1.55 micron light in BP and second, we fabricated a BP FET sample which also showed photoresponse.

Outlook

To improve the BP-Si photodetector photodetector performance we are thinking about different device layouts. Two possible improvements are shown in Figure 15. The left schematic shows a device, in which the source is fabricated as an aluminum electrode instead of using the silicon as an electrode directly. Aluminum is known to form an Ohmic contact with silicon, and therefore, a Schottky-junction can be excluded. This Schottky-junction would show rectifying behavior the same way as the BP-Si junction. The Au electrode is fabricated on top of the BP flake. Measurements showed, that BP forms a poor electrical contact when placed on top of the metal.

Another improvement is shown in the right schematics of Figure 15. Instead of using only an electrode on the side, a graphene sheet could be transferred on top of the BP flake to increase the extraction efficiency of photo-excited carriers.

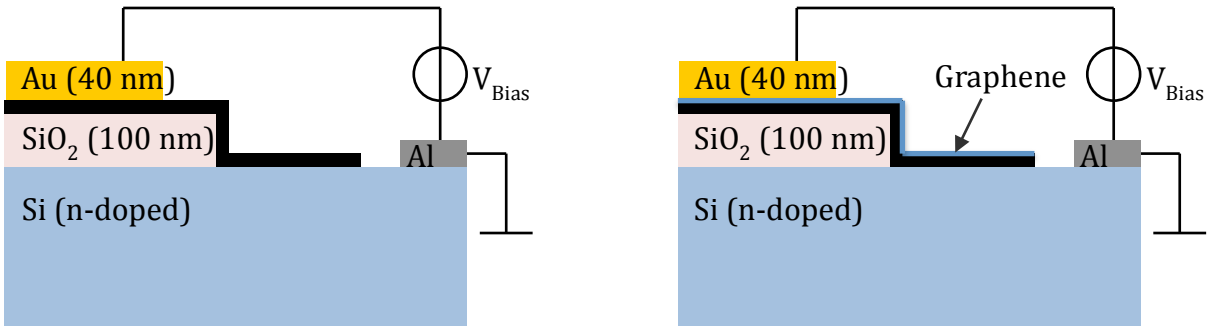

Figure 15: *Further device improvements. Left: Fabricating the metal electrode on top of the BP flake and not vice versa should improve the contact resistance. Additionally an Aluminum electrode is used to contact the Silicon. Right: A graphene sheet can be used as electrode. This layout should lower the contact resistance and improve carrier extraction.*

Both devices are currently in fabrication and measurements will show the actual improvements that can be achieved.

Plasmon-enhanced mid-infrared graphene photodetector

The aim of this project is to fabricate a graphene photodetector, which detects light in the mid-infrared spectral range by exploiting plasmons. Our photodetector is specifically designed for a wavelength of 7.7 µm because of a Quantum-Cascade-Laser (QCL) source available in the lab.

The first experiment was to check if a plasmon can be excited in the desired wavelength range (7.7 µm corresponds to 1298 cm^{-1}). To do so, CVD graphene was transferred to a piece of highly resistive silicon wafer and cut into ribbons by electron beam lithography and subsequent reactive ion etching (RIE). By shining light from a broadband light source (globar) on the sample and measure the spectral absorbance it can be seen, that for a ribbon width of around 100 nm the plasmon resonance appears at the desired wavelength (Figure 16). The resonance strongly depends on the carrier concentration in the graphene sheet and can be shifted by electrostatically doping the sample (Figure 17). Also environmental parameters (e.g. dirt on the sample, humidity in the surrounding air) influences the doping level of the graphene sheet and, therefore, results in a shift in the plasmon resonance.

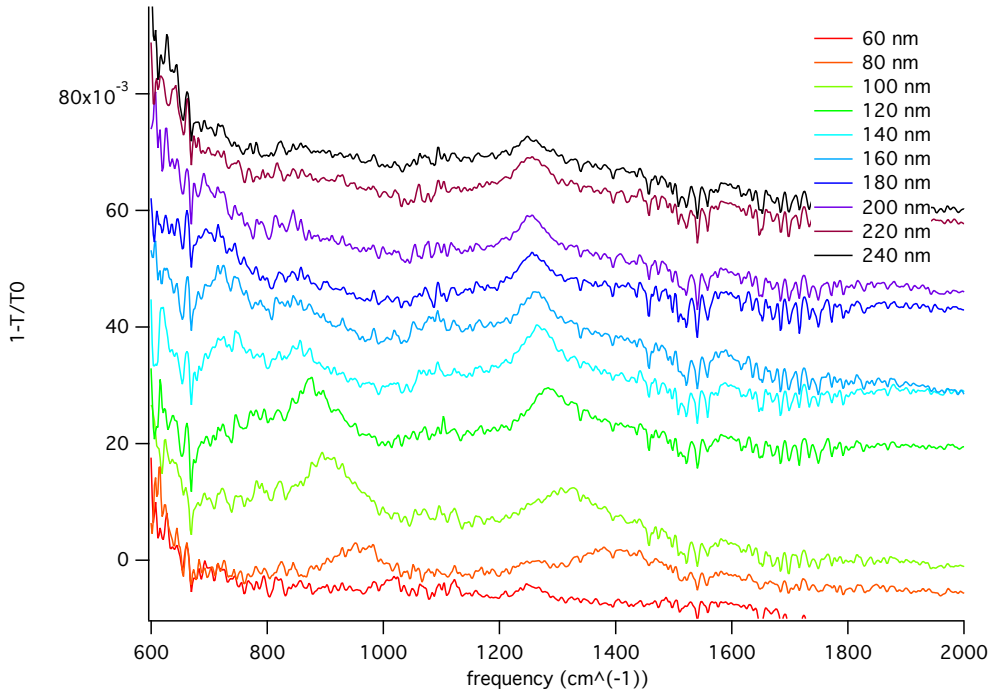

Figure 16: *Transmission Extinction ratio 1-T/T0 for different ribbon width.*

The device layout looks as follows (compare Figure 18): Two gate electrodes (split gates) are used to create a p-n junction across the photodetector. On top of the gate electrodes a dielectric layer (100 nm SiO_2) is deposited and CVD graphene is transferred. After transfer and defining the device area by lithography and RIE etching the two contact electrodes are defined by electron-beam lithography, thermal metal evaporation and lift-off. Another lithography and RIE etching step is necessary to define the nanoribbons.
The actual devices vary from this device scheme in terms of complexity. Because of the large laser spot size (measured to be around 30 micrometer) the device dimensions are also on this scale. The active device area is chosen to be 80x50 microns. As the diffusion

length of photogenerated carriers is much lower than that we fabricated several p-n junctions within the device area. The gate electrodes as well as the source and drain contacts are interdigitated to get a maximum active device length of 5 micron. A scanning electron microscope picture as well as an optical microscope image of the actual device is shown in Figure 19.

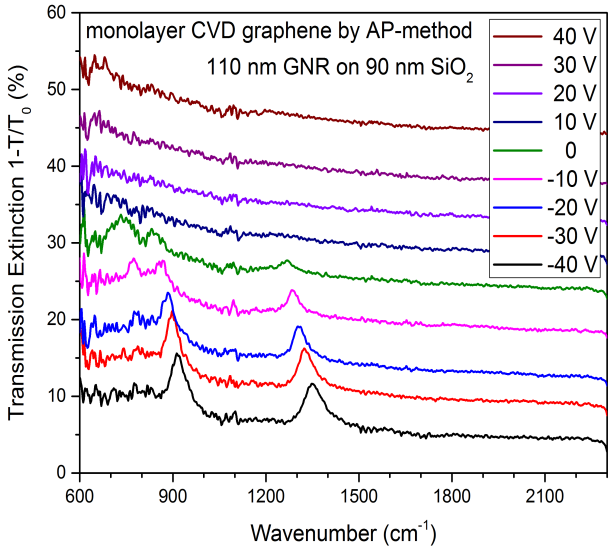

Figure 17: *The plasmon resonance can be shifted by electrostatically doping the graphene sheet.*

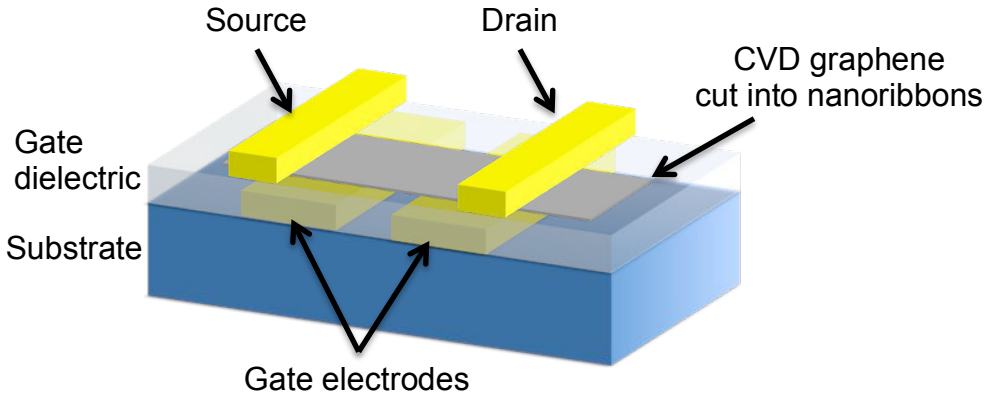

Figure 18*: Schematic device layout of the plamon-enhanced mid-infrared graphene photodetector.*

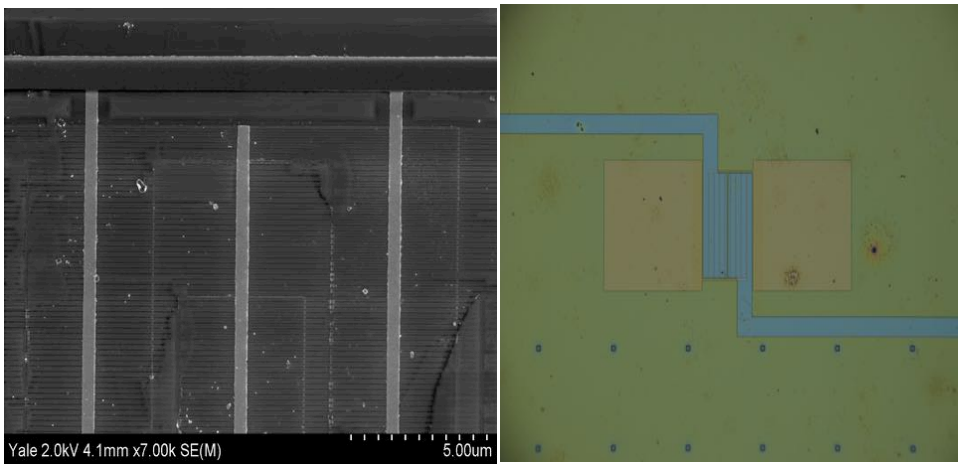

Figure 19: *Scanning electron microscope (left) and optical microscope image (right) image of an actual device*

Conclusion and Outlook

We could achieve to get promising data for all three projects in which I was involved.

For the Graphene-hBN-Graphene sandwich device we clearly see hot carrier emission while shining light on the sample. We could not see any evidence of the negative differential resistance effect that is predicted by Rodriguez-Nieva et al. [15], but we think that a more careful fabrication process and measurements at lower temperatures could lead to that effect. The data on hot carrier emission in such a structure is interesting by itself, as something compareable has, to the best of our knowledge, not been published.

For the black-phosphorus/silicon mid-infrared photodetector it is not completely clear why we could not achieve any light detection in the mid-infrared. We think, again, a more careful fabrication could lead to the desired behavior, but fabrication including black phosphorus is tricky due to its rapid degradation in air and ambient environment. As the bandgap of black phosphorus is small, measurements using longer wavelength laser light can be carried out. This mid-infrared photodetection could make the bP/Si photodetector particularly interesting.

We could show that the plasmon-enhanced mid-infrared graphene photodetector works in principle. An advantage is the usage of large area CVD graphene that enables batch fabrication. During my stay, the first measurements on different devices and device-layouts were done, but a more careful and systematic study to determine the photo-responsivity needs to be carried out. Another problem, which needs to be addressed, is the question on how to dope the graphene nanoribbons to exactly the plasmon resonance. A direct measurement would be preferable, but this is very difficult due to the device layout.

Over all I can summarize that I had a very interesting and productive stay at Xia-Group in Yale. A lot of work is already done and we agreed to continue to work on the projects as well as our collaboration on future projects. At this point I want to thank the people and organizations that made this exchange possible. First of all Professor Thomas Müller for letting me go and Professor Fengnian Xia for accepting me as a visiting scholar in his group. I want to thank all group members at Yale for having a pleasant stay and for the opportunity to learn a lot from them. I also want to acknowledge the financial support of the Austrian Marshall Plan Foundation.

References

[1] Novoselov, K. S. *et al.* Electric field effect in atomically thin carbon films. *Science* **306,** 666–669 (2004).

[2] Novoselov, K. S. *et al.* Two-dimensional atomic crystals. *Proc. Natl Acad. Sci. USA* **102,** 10451–10453 (2005).

[3] Lee, C., Wei, X. D., Kysar, J. W. & Hone, J. Measurement of the elastic properties and intrinsic strength of monolayer graphene. *Science* **321**, 385–388 (2008).

[4] Mayorov, A. S. et al. Micrometer-scale ballistic transport in encapsulated graphene at room temperature. *Nano Lett.* **11**, 2396–2399 (2011).

[5] Nair, R. R. et al. Fine structure constant defines visual transparency of graphene. *Science* **320**, 1308 (2008).

[6] Liao, L. et al. High-speed graphene transistors with a self-aligned nanowire gate. *Nature* **467**, 305–308 (2010) .

[7] Sordan, R. and Ferrari, A.C., "Gigahertz Multi-Transistor Graphene Integrated Circuits." *Technical Digest-International Electron Devices Meeting, IEDM*. (2013).

[8] Xia, F. N., Mueller, T., Lin, Y. M., Valdes-Garcia, A. & Avouris, P. Ultrafast graphene photodetector. *Nature Nanotechnol.* **4**, 839–843 (2009).

[9] Liu, M. et al. A graphene-based broadband optical modulator. *Nature* **474**, 64–67 (2011).

[10] Bonaccorso, F. et al., Production and processing of graphene and 2D crystals. *Materials Today* **15**, 564-589 (2012).

[11] Liu, H. et al., Phosphorene: An Unexplored 2D Semiconductor with a High Hole Mobility. *ACS Nano (in press)* DOI: 10.1021/nn501226z (2014).

[12] Li, L. et al., Black Phosphorus Field-effect Transistors. *arXiv:1401.4117* (2014)

[13] Buscema, M., et al., Fast and broadband photoresponse of few-layer black phosphorus field-effect transistors. *arXiv:1403.0565* (2014).

[14] Xia, F., Wang, H., Jia, Y., Rediscovering Black Phosphorus: A Unique Anisotropic 2D Material for Optoelectronics and Electronics. *arXiv:1402.0270v2* (2014).

[15] Rodriguez-Nieva, J.F. et al., Thermionic Emission and Negative dI/dV in Photoactive Graphene Heterostructures. Nano Lett. **15**(3), 1451-1456 (2015).

[16] Wang, X. et al., "Highly Anisotropic and Robust Excitons in Monolayer Black Phosphorus," *Nature Nanotechnol.*, in press (2015)

[17] Youngblood, N., et al., Waveguide-integrated black phosphorus photodetector with high responsivity and low dark current. Nature Photon., in press (2015)